No. 3230

#3368

Influence of Temperature Stratification on Pressure Differences Resulting from the Infiltration Stack Effect

J.P. Chastain
ASHRAE Student Member

D.G. Colliver, Ph.D., P.E.
ASHRAE Member

ABSTRACT

A two-room environmental chamber was constructed to create environments that could simulate the temperature gradients across a wall and ceiling section of a two-story building. Idealized openings could be mounted in a test structure between the two rooms at 10 different locations. The stratification of air temperature on both sides of the test structure and the differential pressure profiles due to the stack effect were observed for four opening distributions and mean temperature differences ranging from 29°F to 88°F (16°C to 49°C). The temperature stratification on the warm side of the simulated structure was observed to vary from 3.6°F to 15.5°F (2.0°C to 8.6°C). A linear regression analysis was performed on each differential pressure profile to determine if the observed range of temperature stratification had a significant influence on the prediction of the differential pressures resulting from the stack effect. It was determined that the observed temperature stratification did not influence the prediction of the pressure differences. A regression method was developed to determine the elevation of the neutral pressure level and the mean density difference from a single differential pressure profile.

INTRODUCTION

The pressure differences due to the stack effect are considered to be a function of the mean air density difference between the interior and exterior of a structure, and the vertical distance from the elevation of zero pressure difference (i.e., the neutral pressure level). The use of a mean density difference imposes the assumption that the effect of stratification is negligible or stratification of air temperature does not exist either inside or outside a structure. In most situations the assumption that the outside air temperature is non-stratified is a fairly good one. In office buildings that use continuous recirculating mechanical ventilation, the assumption that the internal air in the structure is nonstratified may also be valid. However, in low-rise residential or office structures that do not have continuous air mixing devices, it is expected that the warm air within the structure would be stratified to some extent. Furthermore, in the heating case, the degree of stratification within such a structure would tend to increase as the outdoor temperature decreased. Therefore, situations may exist where the stratification of air temperature within a structure would be a factor in infiltration calculations.

In a recent experimental study (Lee et al. 1985) of the stack effect on a simulated high-rise building it was concluded that a linear relationship, which was derived based on the assumption that temperature stratification did not exist, can be used to correctly predict the pressure differences due to the stack effect. In that study the air temperatures within the experimental structure were carefully controlled by electric heating units placed throughout the height of the structure. Therefore, temperature stratification was not allowed to occur.

The overall purpose of this paper is to describe the construction of a two-room environmental chamber that can be used to simulate actual thermal gradients across a full-scale, two-story wall and ceiling section, and to provide preliminary results from a more comprehensive study of the stack effect on low-rise structures. The specific objectives reported in this paper are:

1. To measure the differential pressure profiles due to the stack effect across a simulated two-story structure over a large range of temperature differences;
2. To observe the corresponding stratification on both the warm and cold sides of the simulated two-story structure; and
3. To determine if the observed range of temperature stratification significantly influences the prediction of the differential pressures resulting from the stack effect.

THEORY

It can be shown from the ideal gas law that a temperature difference across the shell of a structure induces a density difference in the air between the interior and the exterior. A pressure difference profile develops across the envelope of the structure as a result of this density difference. The flow of air induced by these pressure differences is similar to the draft associated with a chimney. Hence, this

J.P. Chastain, Research Specialist, and **D.G. Colliver**, Associate Professor, Department of Agricultural Engineering, University of Kentucky, Lexington.

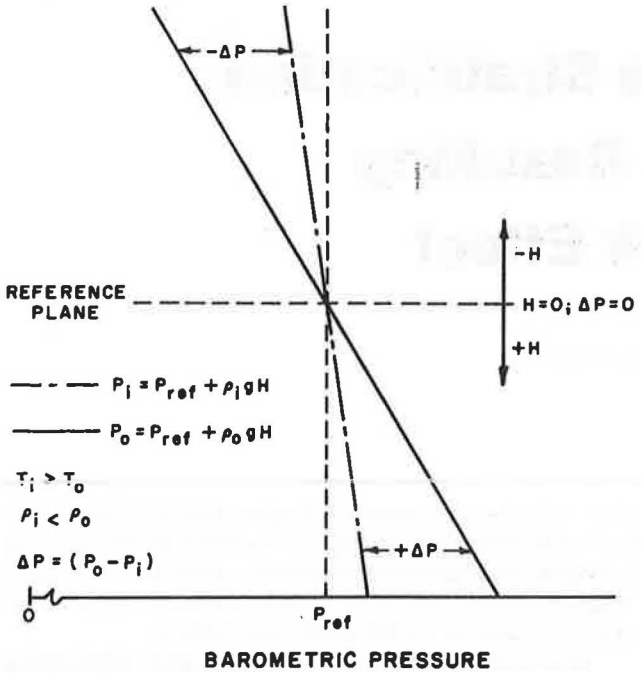

Figure 1 *Theoretical variation of the pressure difference due to the stack effect*

phenomenon is generally referred to as the stack effect (ASHRAE 1985).

The pressure induced by the weight of a column of air at a particular barometric pressure varies with the air density and the elevation. The pressure variation in a static fluid with respect to elevation is described by the following differential equation (Fox and McDonald 1978):

$$dP / dy = - \varrho g \quad (1)$$

where

P = the pressure at a point in the fluid
y = the elevation of the point
ϱ = the air density, and
g = the acceleration due to gravity.

Equation 1 was integrated based on the following assumptions:

1. The air density is constant (i.e., no temperature stratification);
2. The distance from a plane of reference, y_{ref}, is considered positive when measured downward; and
3. The acceleration due to gravity is constant.

Integration and application of the sign convention yields the static fluid equation given by:

$$P = P_{ref} + \varrho gH \quad (2)$$

where

P_{ref} = the barometric pressure at the reference plane, and
H = the distance of a point from the reference plane ($y_{ref} - y$).

The static fluid equation only describes the variation of pressure within a single column of air. The equation that describes the variation of the pressure difference due to the stack effect may be developed by applying the static fluid equation to the volumes of air inside and outside a structure.

$$P_o = P_{ref} + \varrho_o gH \quad (3a)$$

$$P_i = P_{ref} + \varrho_i gH \quad (3b)$$

where

i = inside, and
o = outside

The temperature inside the structure, T_i, is assumed to be greater than the outside temperature, T_o, and both temperatures are assumed to be constant with elevation. Since ϱ_o is greater than ϱ_i, the external pressure is greater in magnitude than the internal pressure at any point below the reference plane.

As shown in Figure 1, the pressure in each volume of air varies with the distance from the reference plane independently. The pressure difference due to the stack effect at any elevation is ($P_o - P_i$). At the reference plane both P_o and P_i are equal to the barometric pressure at the elevation of the reference plane and the pressure difference is zero. Consequently, the pressure difference due to the stack effect is the net pressure difference resulting from the density difference alone. Since the pressure difference at the reference plane is zero, the reference plane is called the neutral pressure level (NPL). Differential pressures are positive below the NPL and negative above the NPL as a result of the sign convention.

The expression for the variation of pressure difference induced by the stack effect is obtained by simply subtracting Equation 3a from Equation 3b.

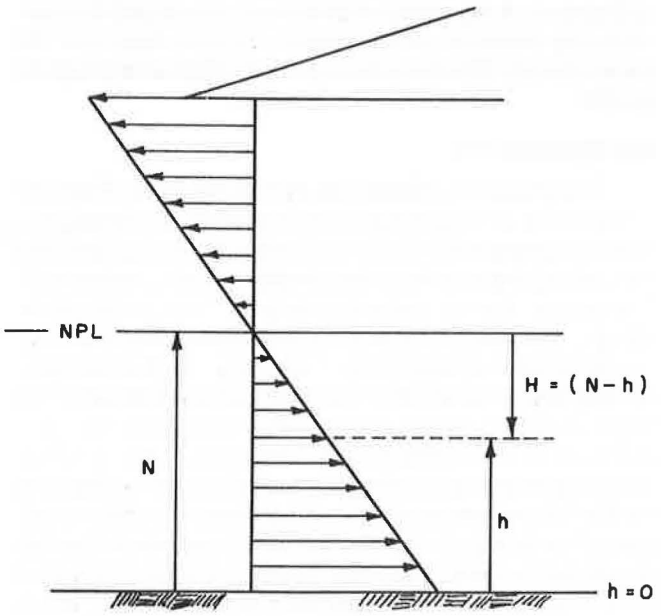

Figure 2 *Distance of a point from the neutral pressure level (H) defined in terms of the elevation of the NPL (N) and the elevation of the point (h)*

$$\Delta P = g\Delta\varrho H \quad (4)$$

where

$\Delta P = (P_o - P_i)$, and

$\Delta\varrho = (\varrho_o - \varrho_i)$.

In the above equation it can be seen that the slope of the linear differential pressure distribution is the product of the acceleration due to gravity and the density difference of the two volumes of air.

A typical differential pressure profile across a wall of a structure due to the stack effect is presented in Figure 2. If the floor of the structure is considered to be at a height of zero, then the distance from the NPL to any point on the envelope may be defined as the difference between the height of the NPL (N) above the floor and the height of the point in question (h). The differential pressure equation may be written in terms of the height above the floor of the structure as follows:

$$\Delta P = g\Delta\varrho(N - h) \quad (5)$$

Many sources express the density difference in terms of either the internal or external air density and the absolute temperatures (ASHRAE 1985; Lee et al. 1985). The density of air is a function of temperature, humidity, and barometric pressure. Cold air (i.e., the outside air) has a much lower moisture-carrying capacity than warm air. Therefore, in an actual heating situation the density of the outside air is simplest to estimate. Using the density of the outside air as the reference, the density difference of Equation 5 may be written as:

$$\Delta\varrho = \varrho_o(1 - \varrho_i / \varrho_o) \quad (6)$$

Application of the ideal gas law gives the following expressions for the densities of the inside and outside air (T_i and T_o are in absolute):

$$\varrho_i = P_{ref} / RT_i, \text{ and } \varrho_o = P_{ref} / RT_o \quad (7)$$

where

R = the ideal gas constant.

Substitution of these expressions into the density ratio of Equation 6 and simplifying results in the following formula for the density difference:

$$\Delta\varrho = \varrho_o(\Delta T / T_i) \quad (8)$$

where

ΔT = the mean temperature difference $(T_i - T_o)$.

Substitution of Equation 8 into Equation 5 gives:

$$\Delta P = g\varrho_o(\Delta T / T_i)(N - h) \quad (9)$$

Equation 9 describes the pressure difference due to the stack effect as a function of outside density, internal and external absolute temperatures, and the distance from the neutral pressure level. The derivation of this equation was based on the assumption that internal and external air densities are constant or that any stratification that may be present does not influence the ΔP distribution. The purpose of the following experiment is to directly test this assumption by observing differential pressures and temperatures as a function of elevation on a simulated two-story wall and ceiling section over a large range of temperature difference conditions.

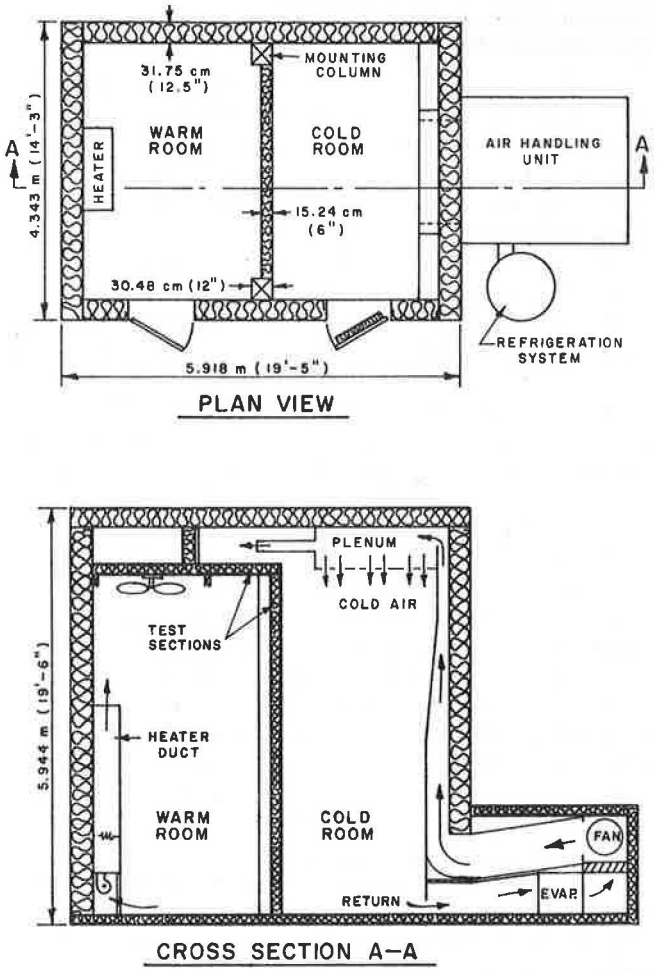

Figure 3 *The two-room environmental chamber*

DESCRIPTION OF THE EXPERIMENTAL APPARATUS

An experimental apparatus was built to produce pressure differences from the difference in the interior/exterior fluid densities and their stratification. A two-room environmental chamber was constructed to simulate the temperature gradients across a test section separating the two rooms of the chamber. The facility was capable of producing mean temperature differences as great as 108°F (60°C) across the removable two-story wall and ceiling sections (refer to Figure 3). The test sections and the exterior walls of the chamber were built as airtight as possible. The wall section had nine locations at various elevations where an idealized opening could be mounted into the wall to simulate structural leakage. The ceiling section had one mounting plate for an idealized opening and a circular mounting plate to enable the study of a chimney at a later date. The two-room environmental chamber was instrumented such that the temperatures on both sides of the test sections and the differential pressures across the test sections could be observed.

Construction of the Two-room Environmental Chamber

The base of the chamber had outside dimensions of 14.25 ft (4.343 m) by 19.42 ft (5.918 m) and the external height was 19.50 ft (5.944 m). The walls were of double-stud wood construction and were 12.5 in (317.5 mm) thick. The ceiling and exterior walls were insulated to about R-42 by filling the cavities with two R-19 fiberglass batts and applying foil-faced foamboard on the interior surface of the framing. The floor of the chamber was constructed of 2 × 6 lumber (16 in o.c.) placed on a concrete slab floor. The cavities between the floor joists were insulated with R-19 fiberglass batts. The cavities beneath the test wall and mounting columns were insulated using extruded polystyrene foamboard to provide a thermal break with an R-value of about 50. The thermal break was installed to prevent excessive heat flow underneath the test wall.

A continuous 4-mil polyethylene vapor retarder was installed beneath the exterior plywood on the walls, beneath the plywood of the chamber floor and over the top layer of insulation on the ceiling. All of the seams in the vapor retarder were overlapped a minimum of 4 ft (1.22 m) and sealed with an adhesive sealant. A second continuous vapor retarder was formed on the interior of the chamber by sealing all of the seams and nail holes in the foil-faced foamboard with foil tape, sealing the joints in the plywood floor and the joint between the foamboard and the floor with silicone caulk, and painting the plywood floor with three coats of polyurethane varnish.

An insulated steel access door was furnished for each side of the environmental chamber. The doors had a foam insulation core that was rated R-14 by the manufacturer and each door was equipped with magnetic seals. An additional 4 inches of foam insulation were added to the access door of the cold room. A large sheet of polyethylene plastic was also taped over the outside of the access door to the cold room while the system was in operation.

The Cooling and Heating Systems

The temperature of the cold room was capable of being controlled between – 25°F (– 32°C) and 65°F (18°C). The cooling was provided by a 5-ton R-502 refrigeration system with a water-cooled, shell-in-tube condensing unit. Partial compressor capacity unloading was provided via hot gas bypass. The refrigeration system was designed to provide 24,000 Btu/h (7.03 kW) of heat removal at a room temperature of – 25°F (– 32°C). Room temperature was controlled by means of an electronic temperature-sensitive suction throttling valve.

The air-handling unit was equipped with a fan that delivered an airflow of 4500 cfm (2.12 m^3/s). This was equivalent to 2.6 air changes per minute in the cold room.

The warm room was equipped with an electric heater that could maintain a room temperature from 50°F (10°C) to 84°F (29°C). A small blower was mounted at the base of the heater duct and delivered an airflow of about 130 cfm (0.061 m^3/s). Four resistance heating elements were mounted downstream from the blower. The output power of the heaters could be varied from 0 to 880 W by means of four variable-voltage transformers (one for each element). The airflow was directed toward the ceiling, where the heated air could be uniformly distributed by means of a variable-speed paddle fan. The chamber was located in a high-bay area of a large laboratory that was heated with steam fan coil units and cooled with natural ventilation.

Description of the Test Sections

A removable wall and ceiling section was constructed between the two permanent mounting columns (shown in Figure 3). The wall section was 10 ft (3.05 m) wide by 16.27 ft (4.959 m) tall. The ceiling section measured 12.17 ft (3.71 m) wide by 9.17 ft (2.79 m) long. The wall and ceiling sections were constructed of 2 × 6 southern yellow pine lumber (24 in o.c.) and the cavities were insulated to a value of R-23 except for the center cavity. Both sides of the center cavity in the test wall and ceiling were covered with removable laminated foam insulation panels. Each panel had an R-value of 11 to give a total of R-22 in the center cavity. When the insulating panels were in place, a 3 in (76.2 mm) cavity was left in the center of the test sections to facilitate the mounting of pressure taps in the test sections and to provide a channel for routing the tubes from each tap to the pressure transducer. The joints and seams between the test sections and the mounting columns were sealed with silicone caulk and foil tape.

Ten plywood plates for mounting openings were built into the test sections, as indicated in Figure 4. Each mounting plate had a 4 in by 20.5 in (101.6 by 520.7 mm) opening and foam weatherstripping was glued around the

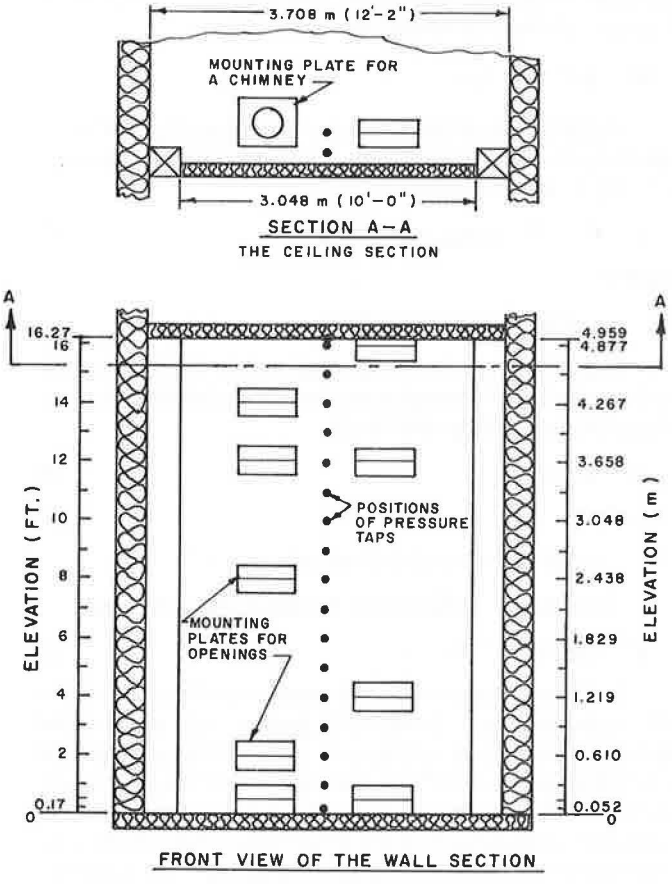

Figure 4 *Schematic of the test sections as viewed from the warm room*

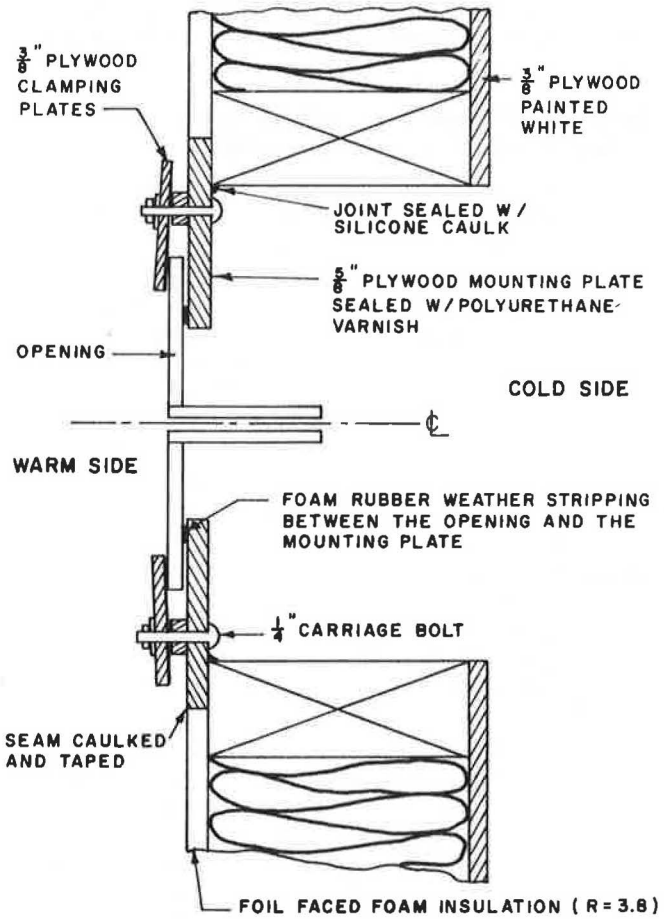

Figure 5 *Profile of a typical opening and the technique used to mount an opening in the test sections*

perimeter of the opening. Extra pieces of weatherstripping were overlapped at the corners to attempt to create a continuous seal. The fabricated openings were held in place by two 3/8 in plywood clamps and six carriage bolts, as shown in Figure 5. The tightening of the plywood clamps with the bolts not only held the center line of the opening at the correct elevation but also created a seal by pressing the flange of the opening against the weatherstripping. When a particular mounting plate was not in use, an insulated plywood cover was clamped over the opening in the mounting plate and a polyethylene sheet covering the entire mounting plate was taped to the test section.

The center line of an opening was marked on each end of the mounting plates. Using these marks as guides, the center line of the opening could be consistently placed at the correct elevation to within approximately ± 1/8 in (± 3.18 mm).

Five straight rectangular openings were used in the experimental investigation. A typical cross section of the openings is evident in Figure 5. All of the openings were fabricated of 0.246 in (6.25 mm) acrylic sheet. The dimensions and flow parameters of the openings are given in Table 1. The cross-sectional area of an opening does not adequately describe the total resistance to flow of an opening. It was shown by Chastain et al. (1987) that the discharge coefficient may be viewed as a dimensionless

TABLE 1
Dimensions of the Idealized Openings

Opening ID.	d (mm)	z (mm)	w (mm)	A (mm²)	γ x10⁻⁴ (m⁻¹)	(Aγ) x10⁻⁵ (m)	C_z	(C_zA) (mm²)
B	1.7	50.8	500.1	850	6.95	.059	.430	366
D	3.3	44.5	500.1	1650	15.36	.253	.696	1148
E	6.3	88.9	499.3	3145	14.60	.459	.747	2349
F	12.9	50.8	498.5	6431	51.98	3.343	.807	5190
G	16.0	123.8	500.1	8002	26.21	2.097	.801	6410

1 in = 25.4 mm

NOTE: The discharge coefficients were computed for each opening using the relationships given in Appendix A with a ΔP = 4.0 Pa, ϱ = 1.224 kg/m³, and ν = 1.436 x 10⁻⁵ m²/s.

flow resistance that is a function of the three-dimensional geometry of the opening ($A\gamma$), the pressure difference, the air properties, and the minor losses, K. The product of the discharge coefficient and the cross-sectional area (C_zA) describes the total resistance to flow of the openings and is the effective opening area. The discharge coefficients given for each of the openings in Table 1 were computed using a pressure difference of 0.016 in H_2O (4.0 *P a) and the air properties indicated. The discharge coefficient equation and the defining relationships for the flow parameters are provided in Appendix A.*

Description of the Differential Pressure Measurements

Twenty pairs of static pressure taps were installed in the test sections at the elevations indicated in Figure 4. Eighteen pairs were mounted in the wall and two pairs were mounted in the ceiling. The pressure taps were fabricated of 1/8 in (nominal, O.D.) copper tubing and were about 2 in (50.8 mm) long. At each measurement elevation, a pressure tap was inserted through a hole in the insulated panels on the warm and cold sides from inside the center cavity of the test sections. The pressure taps were mounted flush with the exterior surfaces of the test sections. The penetrations in the insulated panels were sealed from the interior of the cavity with silicone caulk.

A long piece of flexible, clear, PVC tubing with an outside diameter of 1/8 in was pushed on the end of each pressure tap. The pair of tubes for each differential pressure measurement were the same length and were lightly twisted together. This enabled a pair of tubes to be routed together and any temperature variation in the environment surrounding the tubes would not influence the differential pressure reading. Each pair of tubes came out of the center cavity of the test wall at the elevation of measurement through a small hole in the insulated panels on the warm side of the test wall. The tubes were routed down the surface of the test wall to the pressure transducer, which was located in the warm room.

A single differential pressure transducer was used to measure the pressure difference across the test wall at each elevation. Each pair of tubes was connected to the transducer by means of a manual switching valve. Differential pressure measurements less than 0.0052 in H_2O (1.3 Pa) were accurate within ± 0.0001 in H_2O (± 0.03 Pa) and

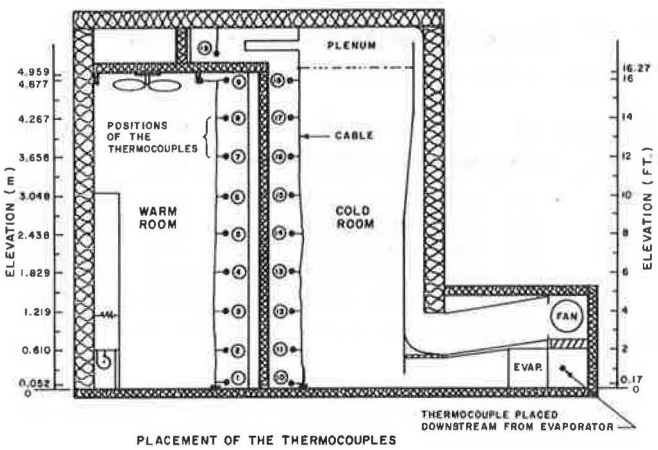

Figure 6 *Positions of the temperature measurements in the cold and warm rooms*

pressure differences greater than or equal to 0.0052 in H_2O (1.3 Pa) could be measured within ± 0.0005 in H_2O (± 0.13 Pa).

During preliminary testing of the instrumentation the cold room was maintained at about – 13°F (– 25°C). The two pressure taps on the cold side of the test ceiling eventually became clogged with ice due to moisture migration through the tubes. The only way to remove the ice was to warm the cold room until the ice melted and then remove the moisture from the tubes by means of a small hand-operated vacuum pump. This procedure proved to be futile because the taps would freeze again after about 24 hours of operation. As a result, the two differential pressure measurements across the ceiling were lost and only the 18 pairs of pressure taps mounted in the test wall were used to gather data.

Description of the Temperature Measurements

The linear expression for the differential pressure given by Equation 5 was based on the assumption that stratification of air temperature does not exist either inside or outside a structure. In order to test the validity of this assumption, temperature measurements were obtained that would not only provide an estimate of the mean temperature in each room but also indicate the temperature variation with respect to elevation.

A temperature-measuring cable was suspended about 2.5 ft (0.76 m) from the center of each side of the test wall (refer to Figure 6). A total of 19 temperature measurements were taken with copper-constantan thermocouples. Thermocouple number 19 was suspended from the ceiling of the cold room in order to measure the air temperature in the semi-enclosed space above the test ceiling. Thermocouples 1 and 10 measured the temperatures at 2.0 in (50.8 mm) above the floor in the warm and cold rooms, respectively. The remaining 16 thermocouples were equally spaced at intervals of 2.0 ft (0.61 m).

The thermocouple leads from the cable in the cold room were passed through a single penetration in the insulated panels (which was sealed with silicone caulk) to the warm room, where all 19 temperatures were recorded using a programmable data logger. The uncertainty of the temperature measurements was estimated to be ± 1°F (± 0.6°C).

Barometric Pressure, Dew Point Temperature, and Wet-Bulb Temperature Measurements

The calculation of the air density in either room required estimates of the dry-bulb temperature, the humidity ratio, and the barometric pressure (ASHRAE 1985). The humidity ratio for the warm room was determined from the wet-bulb and dry-bulb temperatures. The humidity ratio for the cold room was calculated based on measurements of the dew point and dry-bulb temperatures.

The air exiting the evaporator coils was very close to saturation during operation of the refrigeration system since there was no outside air intake and the air turnover rate was high. Therefore, a thermocouple placed downstream from the evaporator (as shown in Figure 6) would indicate a close approximation of the dew point temperature. Since the air-handling system provided 2.6 air changes per minute, the dew point measured downstream from the evaporator would also provide a close estimate of the average dew point temperature in the cold room. The dew point temperature was read with a digital thermometer.

The wet-bulb temperature, which was measured in the warm room using a mechanical psychrometer, was required to estimate the humidity ratio of the air in the warm room.

The standard barometric pressure was obtained on an hourly basis from the Kentucky Weather Wire Service, Bluegrass Airport, Lexington, KY, located approximately 11 miles from the test facility. The elevation of the laboratory floor is 1000 ft (304.8 m) above sea level. The local barometric pressure was determined by subtracting 1.05 in Hg (3556 Pa) from the standard barometric pressure reading.

DESCRIPTION OF THE EXPERIMENT

A series of experiments was performed in the two-room environmental chamber for the purpose of observing differential pressure profiles due to the stack effect and the corresponding degree of temperature stratification in the two rooms. Four opening distributions were used and the mean temperature difference was varied from 29°F (16°C) to 88°F (49°C).

TABLE 2
Definition of the Opening Groups and Vertical Placements

GROUP 1 (G1)		GROUP 2 (G2)		PLACEMENTS H1	PLACEMENTS H2
ID.	Area (mm^2)	ID.	Area (mm^2)	h (m)	h (m)
B	850	E	3145	4.877	3.658
E	3145	G	8002	2.438	4.959*
D	1650	F	6431	0.152	0.152
ΣA = 5645		ΣA = 17578			

* Placement in the ceiling

1 in^2 = 1.550 × 10 ^{3} mm^2

The four opening distributions were defined by combining two groups of openings with two vertical placements. The two opening groups (G1 and G2) and the two vertical placements (H1 and H2) are presented in Table 2. The total cross-sectional area of the G2 openings was roughly three times greater than the G1 openings. Therefore, the two opening groups represented a range of loose and tight construction. It should be noted that the vertical placement designated as H2 involved the placement of an opening in the test ceiling. Reference to Figure 6 indicates that the area above the test ceiling (i.e., on the cold side) was a semi-enclosed space similar to an attic.

Differential pressure and temperature measurements were obtained for the four opening distributions over a range of temperature differences classified as high (72-90°F, 40-50°C), medium (45-54°F, 25-30°C), and low (27-36°F, 15-20°C). These combinations yielded a total of 12 treatments. Furthermore, three data sets were obtained for each opening distribution and ΔT range to give a total of 36 sets of differential pressure and temperature measurements. Ranges of mean temperature differences were used instead of exact temperature differences due to the limitations of the heating and cooling air distribution systems.

The heating system (including the paddle fan) and the cooling system were operated before and after each replication of each treatment, but they were not operated while the differential pressure and dry-bulb temperature measurements were taken. The pressure readings were not taken while the fans were running because the fluctuations in air velocities interfered with the differential pressure readings and the air would not stratify. The heating and cooling systems were operated between each individual test to provide the correct temperature conditions and to break up the residual temperature stratification from the previous test. After the heating and cooling systems were turned off, a period of time was allowed for the mass exchange between the two rooms to come to equilibrium and to allow temperature stratification to occur.

The wet-bulb temperature of the air in the warm room and the dew point temperature of the air in the cold room were measured for each replication. The hourly barometric pressure readings were averaged for each data-taking period.

DATA ANALYSIS AND RESULTS

Observed Temperature Stratification

The average air temperature in the warm room was estimated as the arithmetic mean of nine measurements indicated by thermocouples 1 through 9 in Figure 6. The average temperature in the cold room was estimated as the arithmetic mean of the nine temperatures indicated by thermocouples 10 through 18. The temperature measurement above the test ceiling (provided by thermocouple 19) was not included in the estimate of the average cold room temperature because the air above the test ceiling was often observed to be much warmer relative to the other

TABLE 3
Summary of the Observed Temperature Stratification, ($T_{max} - T_{min}$), in the Warm and Cold Rooms[1,2,3]

OPENING GROUP & PLACEMENT		Warm Room (°C)		Cold Room (°C)			$\Sigma(C_z A)$
	ΔT	T_w	$(T_{max} - T_{min})$	T_c	$(T_{max} - T_{min})$	Above Ceiling	(mm²)
G1H1							
High	48.8	21.4	3.8	– 27.4	3.7	– 23.1	3251
Medium	26.9	22.1	2.4	– 4.8	1.8	– 2.7	2831
Low	20.1*	22.0	2.2	1.9	1.2	2.6	2526
G1H2							
High	47.4	21.8	3.9	– 25.6	3.3	– 14.1	3479
Medium	26.9	22.0	2.5	– 4.9	1.8	.2	3167
Low	16.1	21.8	2.0	5.7	1.1	8.5	2967
G2H1							
High	45.2	20.2	6.8	– 24.9	6.8	– 17.4	13604
Medium	27.3	21.8	4.4	– 5.5	4.2	– 1.1	13303
Low	18.0	22.1	2.5	4.1	2.4	6.7	13073
G2H2							
High	43.7*	18.4	8.6	– 25.4	7.9	– 5.7	13524
Medium	25.3	20.7	4.8	– 4.6	4.1	5.2	13226
Low	16.0	21.5	2.9	5.5	2.1	10.9	12921

* The temperature distributions for these two cases are provided in Figure 7. The differential pressure profiles are compared in Figure 8.

NOTES:

1) The temperature above the ceiling in the cold room is the temperature indicated by thermocouple 19 in Figure 6.

2) The discharge coefficients (C_z) were computed for each opening using the differential pressure and temperature measurements at the opening elevations. The value $\Sigma(C_z A)$ is the sum of the effective opening areas of each opening in the distribution.

3) The data shown for the high and low ΔT cases are the maximum and minimum cases of stratification for the particular opening distribution. The data shown for the medium temperature differences provide an intermediate condition for comparison.

nine measurements. Also, the volume of the space above the test ceiling was small compared with the total volume of the cold room.

The stratification of air temperature in the warm room was calculated as the difference between the maximum and minimum temperatures (i.e., $T_{max} - T_{min}$). The stratification in the cold room was expressed in the same manner except the temperature above the test ceiling was excluded. The data for each opening distribution and temperature difference condition are summarized in Table 3. For brevity, a single data set is provided for each temperature difference condition. All of the data followed the patterns indicated by the data shown. Furthermore, the data for the high and low ΔT conditions correspond to the maximum and minimum cases of stratification for a particular opening distribution. The data set shown for the medium temperature difference condition provides an intermediate level of stratification for comparison.

It can be seen in Table 3 that the temperature stratification in the warm room varied from 3.6°F (2.0°C) to 15.5°F (8.6°C). Excluding the air temperature of the space above the test ceiling, the difference between the maximum and minimum temperatures in the cold room ranged from 2.0°F (1.1°C) to 14.2°F (7.9°C). Generally, the air in the cold room was stratified slightly less than the air in the warm room.

The maximum amount of stratification in both the cold and warm rooms occurred for the distribution G2H2 at the high temperature differences. The minimum stratification in both rooms occurred for G1H1 and G1H2 at the low temperature differences.

To observe the patterns of temperature stratification in both rooms of the environmental chamber the differences between the individual measurements and the mean room temperatures were computed for each data set. Sample distributions for two extreme cases (G1H1 at a low ΔT and G2H2 at a high ΔT) are provided in Figures 7a and 7b. The coolest temperatures in both rooms were near the floor, as expected. The maximum temperatures in the warm and cold rooms were near the ceiling and in the space above the test ceiling, respectively.

Comparison of the temperature distribution in the cold room for the two extreme cases (Figure 7 and Table 3) indicates that the temperature above the test ceiling ranged from 1.3°F (0.7°C) to 35.5°F (19.7°C) greater than the mean room temperature. For the distributions with an opening in the ceiling (represented by G2H2, Figure 7a), the much warmer temperatures above the test ceiling were the result of warm air being discharged through the opening in the ceiling and into this semi-enclosed space. For the distributions without an opening in the test ceiling (represented by G1H1, Figure 7b), the warmer temperatures above the test ceiling were the result of conduction losses across the ceiling from the warm room and poor mixing of air in this space.

An opening was mounted in the test wall at an elevation of 0.5 ft (0.152 m) for each of the four distributions. The cold, dense air that entered the warm room at this elevation was observed (by means of a smoke pencil) to rapidly settle near the floor. Consequently, the temperature near the floor of the room was often much cooler than would be anticipated from the effects of heat transfer alone.

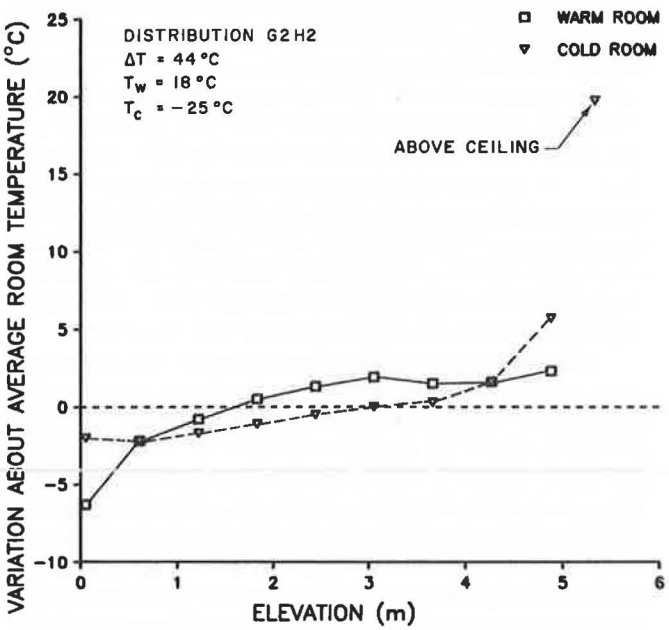

Figure 7a

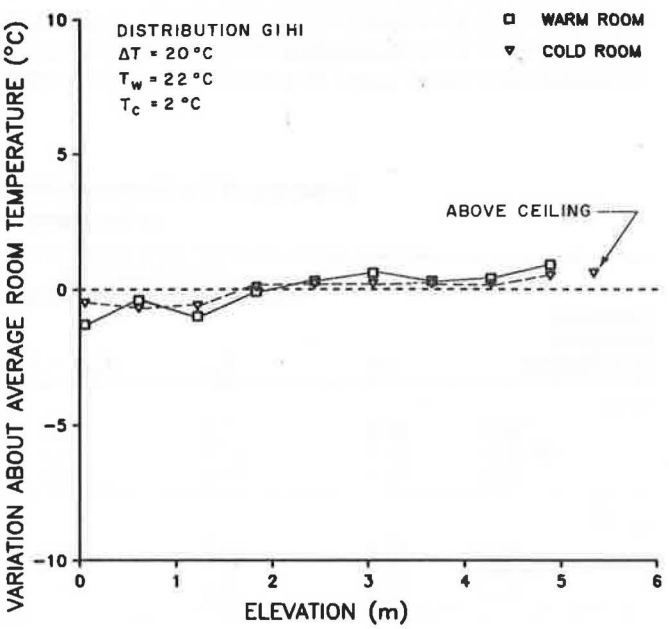

Figure 7b

Figure 7 *Patterns of temperature stratification in the warm and cold rooms for a maximum and minimum case (Figure 7a and 7b, respectively)*

Stratification in the cold room was often greater than would be expected in an actual situation. The air surrounding a two-story structure may typically be considered to be non-stratified due to wind and natural convection effects. Therefore, it would be the stratification of air temperature within a structure that would influence the differential pressures resulting from the stack effect. It was believed that the range of temperature stratification observed for the warm room comprised a range of typical to extreme cases.

Factors That Influenced Temperature Stratification in the Warm Room

Generally, when one considers the factors that influence temperature stratification in a building the following factors affecting the rate of heat transfer from a structure are taken into account: insulating value of the thermal envelope, relative placement of insulation and thermal mass in the envelope, reflectivity of the interior surface, thermal mass of the structure and interior furnishings, and the temperature difference between the interior and exterior. Excluding the temperature difference, an increase in any of these structural variables would tend to decrease the stratification within the structure. The environmental chamber was not typical of most two-story structures because the chamber walls had a large thermal resistance, the interior surfaces were highly reflective, the test wall was insulated more than most low-rise buildings, and there were no internal furnishings. Therefore, the environmental chamber tended to decrease the temperature stratification resulting from heat transfer since there was little radiant exchange between the surfaces.

As was noted previously, the cold air that entered the warm room was observed to rapidly settle to the floor. The air near the floor rose within the warm room as a result of being warmed by the surrounding air mass and surfaces, and to replace the volume of air exfiltrating through the openings in the upper portion of the test sections. Consequently, an increase in the rate of mass exchange between the warm and cold rooms would also be expected to cause an increase in temperature stratification.

The rate of mass exchange between the warm and cold rooms was not measured, but any variable that tends to increase the rate of mass exchange between the two rooms would affect stratification in the warm room. The three variables that could influence the rate of mass exchange between the two rooms of the environmental chamber were the total resistance to flow of the distribution (G1 vs. G2), the vertical placement (H1 vs. H2), and the mean temperature difference.

For purposes of comparison, the total resistance to flow of a distribution of openings may be described by the total effective opening area, $\Sigma(C_z A)$. As was stated previously (and as shown in Appendix A) the discharge coefficient (C_z) of a particular opening varies primarily with the pressure difference and the properties of the air flowing through the opening. The discharge coefficients were computed for each opening in the defined distributions (Table 2) using the measured differential pressures and the air properties (ϱ and ν) of the air at each opening elevation. The cold air properties were used if the opening was below the neutral pressure level (NPL) and the warm air properties were used if the opening was located above the NPL. The total effective opening area, $\Sigma(C_z A)$, was merely the sum of the values of $(C_z A)$ for each opening in the distribution.

Comparing the values of $\Sigma(C_z A)$ in Table 3 with the total opening areas (ΣA) in Table 2 indicates that the total effective opening area of the defined distributions were 23% to 55% smaller than the values of ΣA, depending on the resistance of the individual openings, their placement, and the temperature difference. The magnitude of the total effective opening area of the G1 group of openings was more influenced by variations in ΔT than the G2 group of openings because the discharge coefficients of the smaller openings in the G1 distributions were more affected by the variations in ΔP caused by variations in ΔT. A sensitivity analysis of the discharge coefficient equation is provided by Chastain et al. (1987), which describes in detail the impact of the variation of geometry and pressure differences on the resistance of an opening.

It is apparent from the data presented in Table 3 that the variables with the greatest influence on the amount of stratification were the mean temperature difference and the total effective opening area, $\Sigma(C_z A)$, of the distribution. The vertical placement only appeared to influence the stratification for the distributions involving the G2 openings.

In a practical case, only the stratification of the internal air of a low-rise structure would be of interest. Therefore, the following observations were made from the data of Table 3 concerning the variables that influenced the stratification in the warm room.

1. On the average, an increase in ΔT of 165% caused an increase in the amount of stratification of 95%.
2. An average increase in the total effective opening area (G1 vs. G2) of 337% caused an average increase in stratification of 70%.
3. The variation of the vertical placement of the G1 openings did not have a significant influence on the amount of stratification in the warm room.
4. The variation of the vertical placement of the G2 openings typically increased the amount of stratification by 17%.

Based on these observations it was concluded that the amount of stratification in the interior of a low-rise structure is most influenced by the mean temperature difference and the total effective opening area in the envelope. The infiltration rate generally increases with both increases in ΔT and the total effective opening area. Therefore, the degree of temperature stratification within a structure would be expected to increase as the infiltration rate increases.

Analysis of the Differential Pressure Profiles

The linear differential pressure equation, given in Equation 5, was developed from static fluid theory based on the assumption that the air density internal and external to a structure is constant. It was also noted that the slope of the differential pressure equation is the product of the acceleration due to gravity and the density difference across the shell of the structure.

In the previous sections it was shown that the air in the warm and cold rooms of the environmental chamber was stratified by as much as 15.5°F (8.6°C) and 14.2°F (7.9°C), respectively. As a result, the presence of stratification poses the following questions:

1. Based on theory, how would stratification in the warm and cold rooms be expected to influence the measured differential pressure profiles?
2. Does temperature stratification have a distinguishable effect on the observed differential pressure profile?

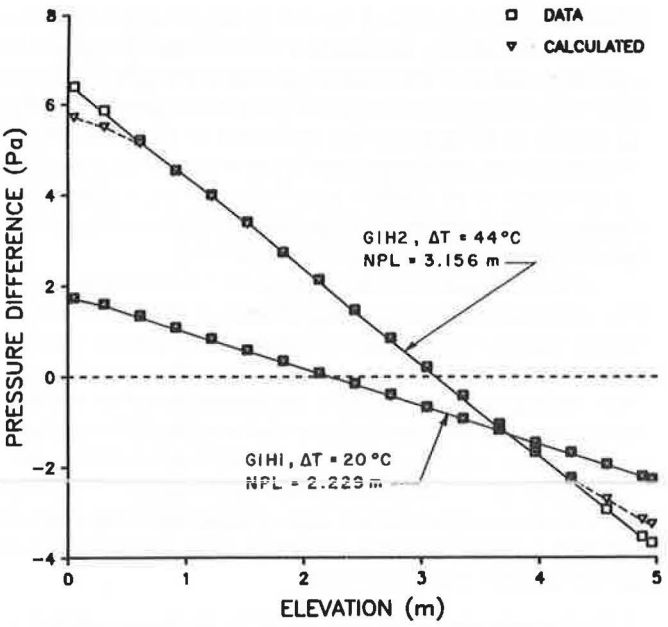

Figure 8 *Comparison of the observed pressure differences with the theoretical values calculated based on the variation of air density in both rooms for two extreme cases of stratification*

3. Should the average density difference or the variation of $\Delta\varrho$ with elevation be used to calculate the pressure differences due to the stack effect for low-rise structures?

These three questions will be addressed by:

1. Comparing the measured ΔP profiles of two extreme cases of stratification with the ΔP profiles calculated based on the anticipated effects of stratification; and
2. Performing a linear regression analysis on each of the 36 measured differential pressure profiles.

Expected Influence of Stratification

The expected variation in the pressure differences resulting from the influence of stratification was computed for two extreme cases of temperature stratification (indicated in Table 3) by applying the following equation at each elevation at which a ΔP measurement was taken.

$$\Delta P = g\,\varrho_c[\,(T_w - T_c)\,/\,T_w]\,(N - h) \qquad (10)$$

where T_w and T_c are the absolute temperatures in the warm and cold rooms at a particular elevation (h), and ϱ_c is the cold air density computed for the same elevation. The values of T_w, T_c, and ϱ_c at the elevations for which temperatures were not measured were obtained by interpolation. The elevation of the neutral pressure level, N, was determined from the differential pressure data (a method to determine the NPL will be presented in a later section).

As was stated previously, maximum and minimum cases of stratification occurred for the distributions G2H2 at a high ΔT and G1H1 at a low ΔT. The measured differential pressures for these cases are compared with those calculated (using Equation 10) in Figure 8. It is apparent from the calculated values in the figure that the primary anticipated effect of stratification in the warm and cold rooms would be to cause a lower density difference near the floor and the ceiling. This is indicated by the lower calculated pressure differences near the floor and ceiling for the maximum case of stratification. The measured ΔP profile for the maximum case of stratification, given by the distribution G2H2, did not indicate any curvature near the ceiling or floor that would indicate the influence of stratification. Neither the calculated nor the measured ΔP profiles for a minimum case of stratification (G1H1 at a low ΔT) indicated any influence of temperature stratification.

Regression Analysis of the Differential Pressure Profiles

The differential pressure data for each replication of each treatment were fit to an equation of the following form:

$$y = a + bx \qquad (11)$$

The independent variable (x) was the elevation of the differential pressure measurement and the dependent variable (y) was the pressure difference. In addition to the coefficient of determination (r^2), the following calculations were performed on each of the ΔP profiles:

1. The differential pressures were predicted from the regression equation;
2. The differences between the observed and predicted differential pressures were computed (i.e., error in prediction or residuals); and
3. The 95% prediction intervals were computed about each predicted value of ΔP.

The equations used to compute the coefficient of determination, the 95% prediction interval, the slope (b), and the y-intercept (a) were the standard equations given in most statistical methods texts (e.g., Younger 1979). Each 95% prediction interval was based on an estimate of the variance about each individual regression line with 16 degrees of freedom.

There was a very high degree of linear correlation between the pressure differences and the elevation of measurement. The 36 coefficients of determination (r^2) ranged from 0.9992 to 0.9999. It was noted that the value of r^2 did not decrease as the temperature stratification increased. Many of the cases with large amounts of stratification had the highest degrees of correlation.

It was determined that only 0.8% (5 out of 648 points) of the errors in prediction of ΔP were outside of their respective 95% prediction intervals. Using a 95% prediction interval one would expect 5% of the predictions to be outside this band of error. However, all of the errors that were outside of the 95% prediction intervals were within the band of error associated with the uncertainty of the differential pressure measurements. A comparison of the errors in the prediction of the pressure differences with the 95% prediction intervals is presented for two extreme cases of stratification in Figure 9. Generally, all of the pressure differences in the 36 ΔP profiles were predicted within $\pm$ 0.0004 in H_2O ($\pm$ 0.1 Pa) using the linear model (Equation 11).

It can be seen that the slope (b) and the y-intercept (a) of the linear regression equation (Equation 11) had physical significance by expanding Equation 5 to give:

$$\Delta P = \Delta\varrho g N - \Delta\varrho g h \qquad (12)$$

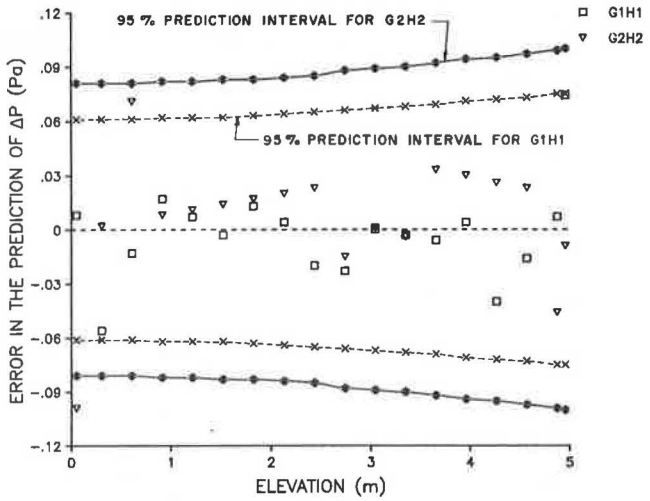

Figure 9 *Comparison of the error in prediction of P and the 95% prediction intervals (P.I.) for a maximum (G2H2) and minimum (G1H1) case of temperature stratification*

Comparing Equation 11 with Equation 12 indicates that the magnitude of the slope of the regression equation was equal to the product of the mean density difference between the warm and cold rooms and the acceleration due to gravity. Also, the slope was always negative due to the sign convention of Figure 2. The y-intercept was the product of the slope and the elevation of the neutral pressure level (NPL).

According to theory (Equation 8), the magnitude of the slope of the differential pressure profiles may be calculated based on the ideal gas law as,

$$slope = \Delta\varrho g = \varrho_c \, (\Delta T / T_w) g \qquad (13)$$

where

ϱ_c = the average air density in the cold room;
ΔT = the average temperature difference between the warm and cold rooms; and

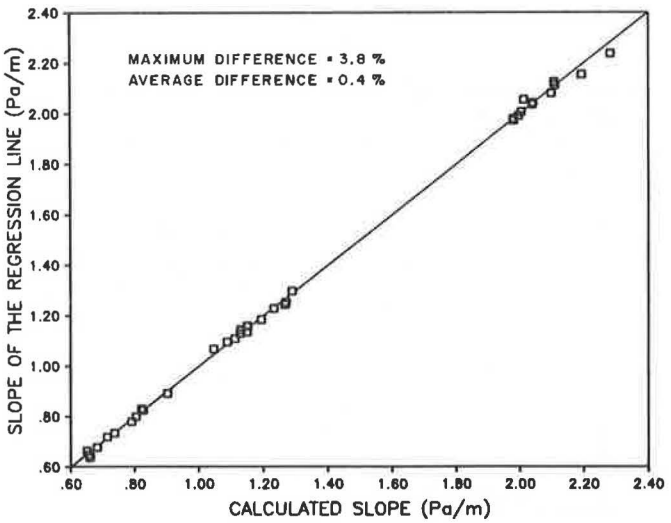

Figure 10 *Comparison of the magnitudes of the theoretical slopes of the differential pressure profiles (calculated using Equation 13) with the values obtained by regression*

T_w = the average warm room temperature (absolute scale).

The advantage of using the ideal gas law approximation for the density difference in Equation 13 is that it eliminates errors involved in attempting to calculate the warm air density. The density of the warm air would be more affected by errors in the estimation of moisture content than the cold air. The slopes of the 36 ΔP profiles were calculated using Equation 13. A comparison of these theoretical values with the magnitudes of the values obtained by regression is presented in Figure 10. The results indicate that the slope of the regression line was in good agreement with the values calculated from theory. The maximum difference was 3.8%, which occurred for G1H2 at a temperature difference of 29.0°F (16.1°C). The magnitude of the slope at this point was 0.0008 in H_2O/ft (0.636 Pa/m). The average difference between the two methods was 0.4%.

Based on the results of the analysis of the differential pressure profiles it was concluded that the observed stratification in the two rooms of the environmental chamber did not have a distinguishable influence on the pressure differences resulting from the stack effect. Thus, the variation of $\Delta\varrho$ with respect to elevation may be neglected for two-story structures subjected to the observed ranges of temperature stratification. Furthermore, the slope of the differential pressure profile may be calculated based on the ideal gas approximation (Equation 13).

Regression Method to Determine the Density Difference and Elevation of the NPL

The high degree of linear correlation and the good agreement between the theoretical values of the slope and the values obtained by regression indicate that linear regression may be used to determine the density difference and elevation of the NPL (N). The density difference and elevation of the NPL were determined from the slope and intercept of the regression equation (Equation 11) in the following manner:

$$\Delta\varrho = | \, b / g \, | \qquad (14)$$

$$N = | \, a / b \, | \qquad (15)$$

The use of the regression method facilitated the computation of 95% confidence intervals about N and $\Delta\varrho$. These confidence intervals were considered analogous to uncertainties of measurement. Since the mean density difference was equal to the slope (b) of the regression line divided by a constant (g), the 95% confidence interval for $\Delta\varrho$ was equal to the standard 95% confidence interval about b on a percentage basis. The 95% confidence interval about N was computed using an equation adapted from a method given by Snedecor and Cochran (1980). A summary of all of the regression equations used has been provided by Chastain (1987).

Application of the regression method to the 36 data sets yielded values of N ranging from 6.73 ft (2.050 m) to 11.99 ft (3.655 m). The 95% confidence intervals about the elevation of the NPL ranged from ± 0.28 in (± 7 mm) to ± 0.98 in (± 25 mm). The mean density difference in-

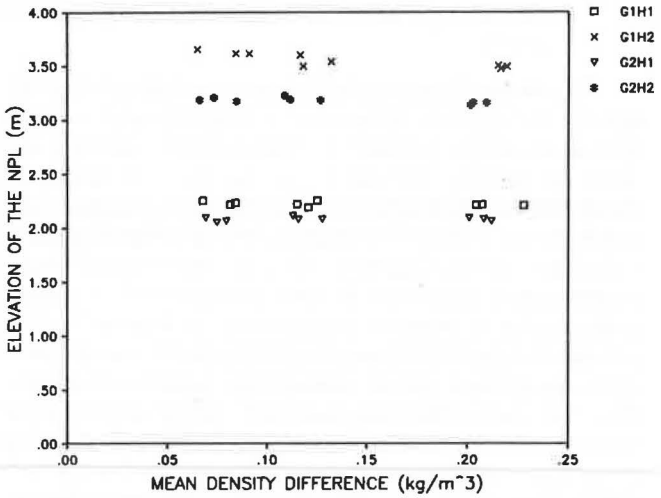

Figure 11 *Variation of the NPL with respect to the mean density difference (values obtained by the regression method)*

creased with the mean temperature difference from 0.0041 lb_m/ft^3 (0.0649 kg/m^3) to 0.0142 lb_m/ft^3 (0.2229 kg/m^3). The 95% confidence intervals about $\Delta\varrho$ ranged from $\pm 2 \times 10^{-5}$ lb_m/ft^3 ($\pm$ 0.0004 kg/m^3) to $\pm 1.3 \times 10^{-4}$ lb_m/ft^3 ($\pm$ 0.0021 kg/m^3).

It is believed that the estimate of the mean density difference by the regression method had the following advantages:

1. The slope of the regression equation was able to respond to the variation of the local barometric pressure between tests;
2. The slope of the regression equation reflected the influence of the actual mean temperatures and moisture contents of the air in both rooms; and
3. The regression method permitted the calculation of a statistical band of error about the estimate of $\Delta\varrho$.

A plot of the observed elevations of the NPL with respect to the mean density difference is presented in Figure 11. The data indicate that the elevation of the NPL was not a function of the mean density difference. Since the mean density difference largely depends on ΔT, the data tend to reinforce the conclusion by Lee et al. (1985) that the elevation of the NPL is not a function of the mean temperature difference. Based on the average for each distribution, the elevation of the NPL varied from 6.82 ft (2.078 m) to 11.66 ft (3.555 m) depending on the size of the openings in the distribution (i.e., G1 or G2) and the vertical placement (i.e., H1 and H2). These observations support the following conclusions presented by Emswiler (1926) and Lee et al. (1985):

1. The elevation of the NPL is a structure-dependent parameter; and
2. The elevation of the NPL for a particular structure is a function of the relative size of the openings in the envelope, their resistance to flow, and their vertical placement.

A detailed analysis of the factors that influence the elevation of the NPL and a method to predict the elevation of the NPL for a particular distribution of openings is beyond the scope of this paper. Such analyses are provided by Chastain (1987), and these topics will be the subjects of future papers.

CONCLUSIONS

The following conclusions were drawn from the data and the results of the regression analysis on the differential pressure profiles:

1. The variation of differences in density induced by the observed temperature stratification did not have a significant influence on the pressure differences due to the stack effect.
2. The differential pressures across the envelope of a two-story structure due to the stack effect may be computed using Equation 9, provided the elevation of the neutral pressure level (NPL) is known.
3. The slope of the differential pressure profile resulting from the stack effect is a function of the temperature difference across the envelope of a structure.
4. The temperature stratification within the warm room of the environmental chamber was influenced most by the mean temperature difference and the total effective opening area mounted in the test sections. Therefore, the degree of temperature stratification within a structure would be expected to increase as the infiltration rate increases.
5. The elevation of the NPL is a structure-dependent parameter that is independent of the temperature difference and the resulting mean density difference across the building envelope.

REFERENCES

ASHRAE. 1985. *ASHRAE handbook — 1985 fundamentals.* Atlanta: American Society of Heating, Refrigerating, and Air-Conditioning Engineers, Inc.

Chastain, J.P. 1987. "Pressure gradients and the location of the neutral pressure axis for low-rise structures under pure stack conditions." Unpublished Masters Thesis, University of Kentucky.

Chastain, J.P.; Colliver, D.G.; and Winner, P.W. 1987. "Computation of discharge coefficients for laminar flow in rectangular and circular openings." *ASHRAE Transactions*, Vol. 93, Part 2B, pp. 2259-2283.

Emswiler, J.E. 1926. "The neutral zone in ventilation." *ASHVE Transactions*, Vol. 32, pp. 59-74.

Fox, R.W., and McDonald, A.T. 1973. *Introduction to fluid mechanics*, 2nd ed. New York: John Wiley and Sons, Inc.

Lee, K.H.; Lee, T.; and Tanaka, H. 1985. "Thermal effect on pressure distribution in simulated high-rise buildings: experiment and analysis." *ASHRAE Transactions*, Vol. 91, Part 2A, pp. 530-544.

Snedecor, G.W., and Cochran, W.G. 1980. *Statistical methods.* 7th ed. Ames, IA: The Iowa State University Press.

Younger, M.S. 1979. *A handbook for linear regression.* Duxburg Press, MA.

ACKNOWLEDGMENTS

This paper is published with the approval of the director of the Kentucky Agricultural Experiment Station and is designated paper No. 87-2-265.

APPENDIX A

RELATIONSHIPS USED TO COMPUTE THE DISCHARGE COEFFICIENTS

The discharge coefficient may be computed from the following relationship (Chastain et al. 1987):

$$1 / C_z^2 = K + \{ 2K / [(1 + (A\gamma)^2 \, 128K\Delta P / \varrho\nu^2)^{0.5} - 1] \} \quad \text{(A-1)}$$

where

C_z = the discharge coefficient,
ϱ = air density,
ν = kinematic viscosity,
K = total minor loss coefficient,
ΔP = total pressure drop across the opening,
A = cross-sectional area, and
γ = a geometric parameter.

The geometric parameter, γ, for a rectangular opening is defined by the following expression,

$$\gamma = \alpha / Bz(1 + \alpha)^2 \quad \text{(A-2)}$$

where

α = aspect ratio = d/w
d = opening thickness
w = opening width
z = flow length, and
B = friction coefficient.

For a rectangular opening the friction coefficient is a function of the aspect ratio. The following relationship may be used to calculate friction coefficients for aspect ratios from zero to 0.075 (Chastain et al. 1987)

$$B = 96.0 - 106.67\alpha \quad \text{(A-3)}$$

The total minor loss coefficient, K, includes losses due to entrance and exit effects. A value of 1.5 was used for the calculations in this paper.